Journal of Geosciences, Osaka City University
Vol. 48, Art. 9, p. 143–158, March, 2005

Event deposits associated with tsunamis and their sedimentary structure in Holocene marsh deposits on the east coast of the Shima Peninsula, central Japan

Hisayo OKAHASHI[a]*, Moriaki YASUHARA[a, b], Muneki MITAMURA[a], Kotaro HIROSE[a] and Shusaku YOSHIKAWA [a]

[a] Department of Biology and Geosciences, Graduate School of Science, Osaka City University, Sugimoto3, Sumiyoshi-ku, 558-8585, Osaka, Japan
[b] Research Fellow of the Japan Society for the Promotion of Science
* Corresponding author. E-mail: hisayo@sci.osaka-cu.ac.jp

Abstract

In Japan, many earthquakes have occurred during historic times. Many tsunamis caused by these earthquakes are recorded in ancient documents. Some researchers have studied tsunami deposits in lake and marsh sediments in coastal areas of Japan.

However there are only very few studies on tsunami deposits at the Kii Peninsula. The coastal area of this peninsula faces the Nankai Trough. Tsunamis triggered by great Tokai and/or Tonankai Earthquakes ($M \geq 8$), whose source is distributed along the Nankai Trough, have been causing serious damage to this area.

We examined some cores related to some event deposits (sand layers) possibly caused by the Tokai and/or Tonankai Earthquakes. Studied cores (A0–6, B1, P1–2) were excavated at the coastal marsh in the east side of the Kii Peninsula. In this marsh deposits, some researchers reported diatom, foraminifera, radiocarbon age and general lithofacies. We summarized these previous studies and carried out detailed lithofacies descriptions and additional radiocarbon dating to elucidate paleoenvironments of the studied area and origin of sand layers.

Temporal changes of Holocene depositional environments of the studied area were elucidated as follow: Around 7,000 cal yr BP, marine (inner bay) environment; ca. 6,500–3,000 cal yr BP, fresh-water marsh; ca. 3,000–1,000 cal yr BP, influence of marine water to the marsh; after ca. 1,000 cal yr BP, fresh-water marsh; the Edo Period– the beginning of the Showa Period, the paddy cultivation in studied marsh; After the beginning of the Showa Period, fresh-water marsh (stopping of the paddy cultivation).

Lithofacies and distribution of event deposits strongly suggested that sand layers were formed by tsunamis.

Key-words : tsunami deposits, Tokai and Tonankai earthquake, Kii Peninsula, Holocene

1. Introduction

Past natural disasters have left their traces as event deposits in the sediment. Recently, many researchers have studied event deposits formed by tsunamis caused by large earthquakes or landslides on the seafloor, i.e., "tsunami deposits" (e.g., Atwater, 1987; Atwater et al., 1995; Dawson et al., 1995; Benson et al., 1997).

It is difficult to predict future natural disaster from

observations in a restricted period of time. Although ancient documents provide important information for the prediction, they are restricted either locally or historically, and may lack credibility. Geological studies of sediments deposited by tsunamis are important because such studies enable us to identify past tsunamis that took place not only in historical age but also in pre-history. If researchers carried our many and detailed studies about tsunami deposits in various areas, our knowledge of the frequency and magnitude of tsunamis will extend largely. The accumulation of more detailed and higher-resolution studies will lead us to the prediction of future tsunamis.

Many earthquakes have been occurred in historic times in Japan. Many tsunamis caused by these earthquakes are recorded in ancient documents. Some researchers have studied tsunami deposits in lake and marsh sediments in coastal areas of Japan (e.g., Nanayama et al., 2003, Pacific coast of Hokkaido; Fujiwara et al., 1997, 1999, 2000, Tsuji et al., 1998, Pacific coast of Honshu Island; Minoura et al., 1987, Japan-Sea coasts of Honshu Island).

However there are very few studies on tsunami deposits at the Kii Peninsula (Tsuji, 1999; Tsuji et al., 2001, 2002). The coastal area of this peninsula faces the Nankai Trough. Tsunamis triggered by great Tokai and/or Tonankai Earthquakes ($M \geq 8$), whose source is distributed along the Nankai Trough, have been causing serious damage on this area (Watanabe, 1998).

Here we examine some cores related to some event deposits possibly caused by the Tokai and/or Tonankai Earthquakes. The studied area is the coastal marsh in the east side of the Kii Peninsula and is situated in the dangerous area for tsunami hazards defined by Aida (1988). Thus, this area is suitable for the study on the historical record, interval and cycle of tsunami inrushes on the basis of geological analysis of tsunami deposits. In these marsh deposits, some researchers reported diatom, foraminifera, radiocarbon age and general lithofacies (Mitamura et al., 2001; Okahashi et al., 2001a, b, 2002; Hirose et al., 2002; Yoshikawa et al., 2003). Thus we summarize these previous studies, and carry out detailed lithofacies description and focused on lithofacies and distribution of tsunami deposits. Aim of this study is to elucidate paleoenvironments of the studied area and origin of sand layers.

2. Study site

The marsh in the Toba City, study area, is located on the central part of the cape located on the east coast of the Kii Peninsula (Fig. 1). The altitude of this small marsh (longer axis: 300–400 m) is at less than 1 m elevation and is surrounded by hills and coastal terraces at about 30 m elevation. There are no large streams entering the marsh. Thus the supply of fluvial sediment is very limited. This marsh is separated by the barrier beach from the seashore. This barrier beach has about 100 m width, less than 2.5 m elevation and NE-SW direction. The marsh was drained and have used for cultivation since well before the 19th century (Toba City, 1991) although only a small part of this marsh is used for cultivation now.

In hills around the studied area, the Mesozoic Matoya Group (Yamagiwa and Saka, 1967), the interbeds of sand and clay stones, is distributed. In gently sloping hills at the elevation of less than 15 m, the Pleistocene Sakishima Formation (Otsuka, 1928a, b), sandy gravel is distributed. In coastal terraces at the elevation of about 20 m, Upper Pleistocene terrace deposits consisting of sandy gravel beds are distributed. The beach ridge, developed along the seacoast, consists of sandy gravel.

Ten cores were obtained at three sites in the marsh. Site P is in the pond at east part of the marsh (for a distance of 150 m from the barrier beach). Site A is at central part (for a distance of 200 m from the barrier beach). Site B is at western part (for a distance of 350m from the barrier beach).

3. Method

Studied cores were taken from the marsh using a "Geo-Slicer" (Nakata and Shimazaki, 1997), that is 30-cm-wide and 10-cm-thickness. Seven cores were taken perpendicular to the shoreline at approximately 5–10 m intervals in Site A (hereafter referred to as A0–A6), two cores were taken in Site P (P1–P2) and one core was taken in Site B (B1). Preliminary lithofacies observation of all cores was carried out in the field. After that, additional lithofacies observations such as texture, structure, color, fossils and grain size were conducted in detail with a binocular microscope in the laboratory.

The length of each core collected in site A is 372 cm (A0), 375 cm (A1), 352 cm (A2), 340 cm (A3), 281 cm (A4), 366 cm (A5) and 570 cm (A6). The length of B1 core is 580 cm. The length of each core collected in site P is 286 cm (P1) and 330 cm (P2).

4. Lithofacies

Lithofacies at three sites (A, B and P) are very similar each other: they consist primarily of mud and intercalating sand layers. These sand layers in cores at site A are correlated between cores and numbered from the top (OS-

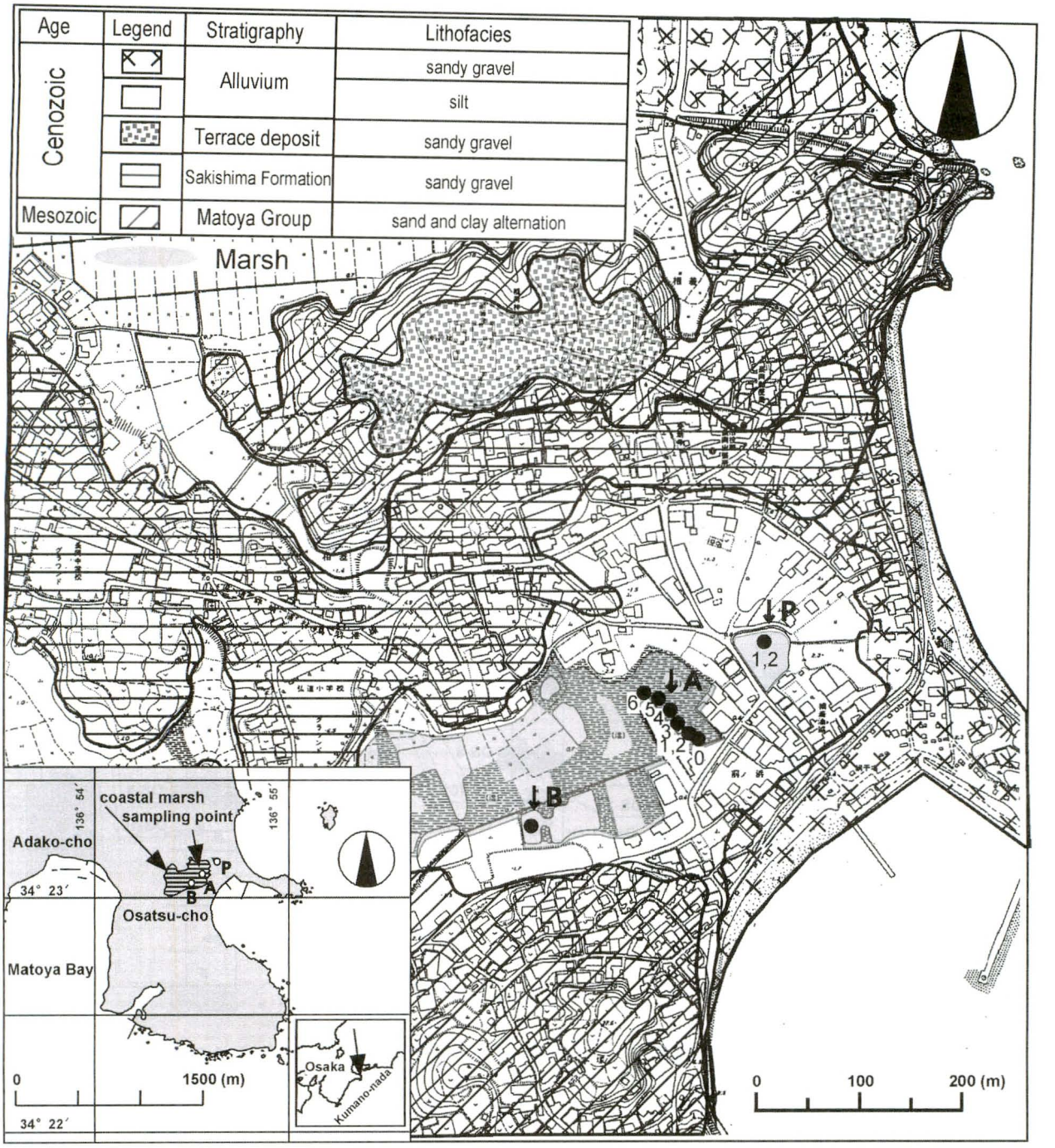

Fig. 1 Index, locality and geological maps.

1–12) by Okahashi et al. (2001a).

The correlation of sand layers between sites A, B and P was carried out by Mitamura et al. (2001) on the basis of similarities of lithofacies [i.e., sedimentary structure (e.g., fining upward sequence) and contents (e.g., molluscan shells, foraminiferal tests, rip-up clasts and/or gravel)] and stratigraphic position of colored mineral concentrated layer. The detailed lithofacies is as follows (Figs. 2–4).

4.1. Site A

Lithofacies of obtained cores in this area can be divided into three parts based on the sedimentary facies, i.e., the lower part (massive sandy gravel layer as the basement rock of this area), the middle part (marine sand overlying the basement rock unconformably) and the upper part (mud with organic fragments, intercalating more than 10 sand or sandy gravel layers)(Fig. 2).

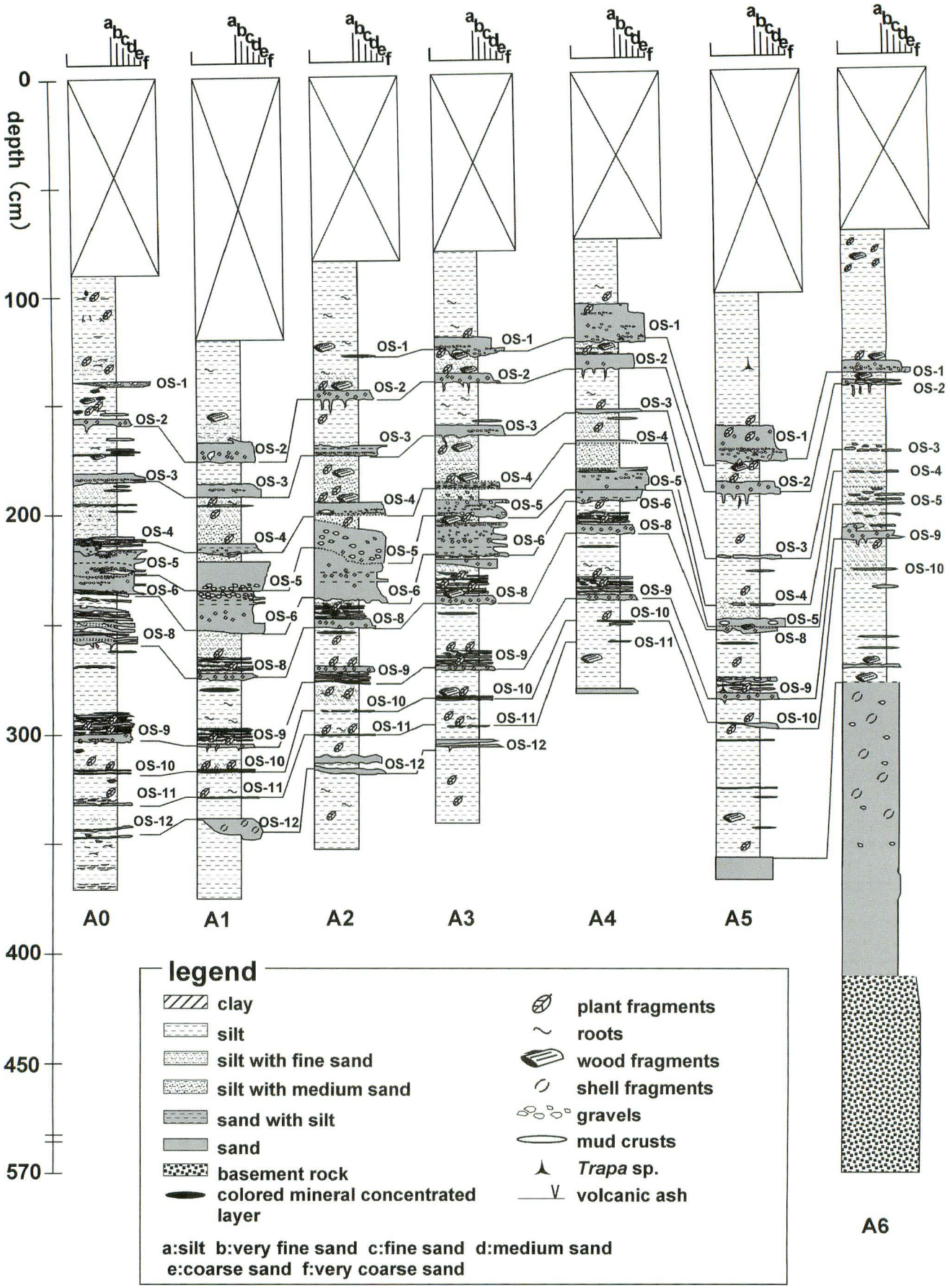

Fig. 2 Geological column of cores in the site A.

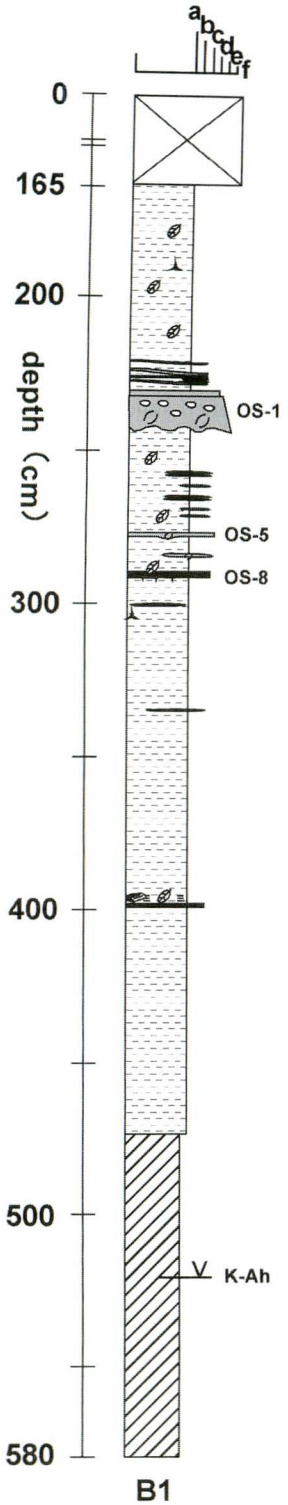

Fig. 3 Geological column of the core in the site B.
Legend of geological column is shown in Fig. 2

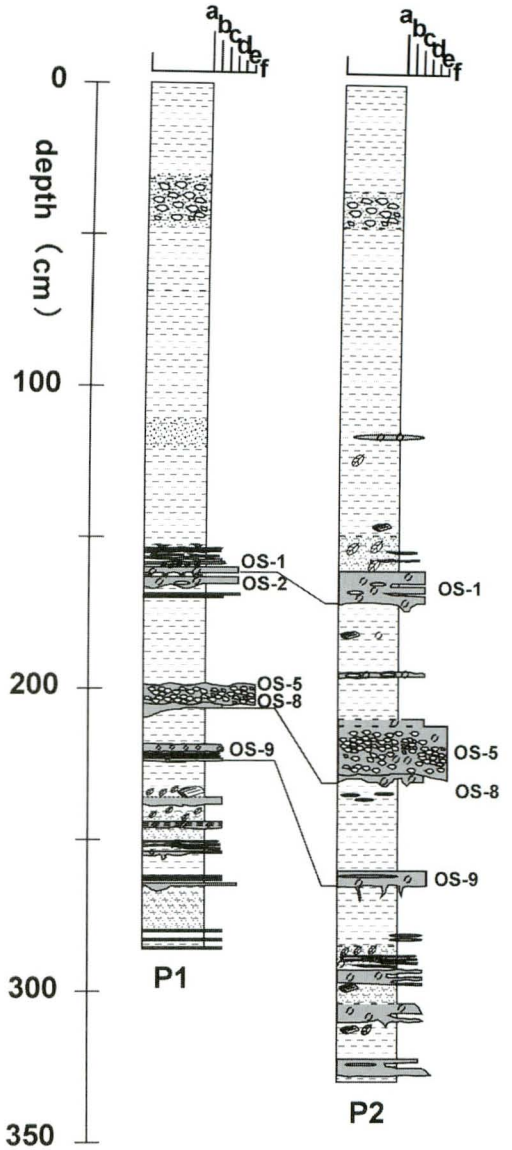

Fig. 4 Geological column of cores in the site P.
Legend of geological column is shown in Fig. 2

4.1.1. The upper part

This part is found in all cores and constitutes the main part of cores. Its thicknesses are 4–5 m through all cores (A0–A6). This part is composed of organic-rich silt and sandy silt, including many sand layers. Its color is brownish-black to grayish-brown. This part is overlain by artificial reclaimed layer for cultivation.

Many sand layers are present in this part. These sand layers have a range in thickness from a few millimeters to more than 20 cm, including rip-up clasts, molluscan shells and plant fragments in many cases. These sand layers have a wide-range and continuous distribution and become thinner landward in many cases. The distal parts of them have a discontinuous (patchy) distribution. There are 11 sand layers (OS 1–12: see Fig. 2) that are recognized in most cores, i.e., these sand layers have a wide-range and continuous distribution. Colored mineral concentrated layer is present in the silt between OS-8 and 9. Detailed profiles of each sand layer are described as follows.

OS-1: This sand layer is found in all cores except the core A1. Its thicknesses are within 17 cm. The thickness of this sand layer in each core is 2 cm (A0), the lens-shape of 1 cm or less (A2), 8 cm (A3), 17 cm (A4), 15 cm (A5) and 5 cm (A6). This sand layer consists of two units. Lower unit is composed of coarse to very coarse grained sand, and upper unit is composed of fine to medium grained sand. Both units show fining-upward sequence respectively. Their color is gray to black. Gravels, plant fragments and rip-up clasts are included around the boundary between upper and lower units. Molluscan shells are included around this boundary in two cores (A4, A5). Contacts between lower beds are sharp and commonly erosional. The silt enclosing this sand layer contains many plant fragments. Especially in the core A6, plant fragments are laminated just above this sand layer.

OS-2: This sand layer is found in all cores. Its thicknesses are 2–9 cm. The thickness of this sand layer in each core is 3 cm (A0), 9 cm (A1), 4 cm (A2), 4 cm (A3), 7 cm (A4), 6 cm (A5) and 2 cm (A6). This sand layer is composed of fine to medium grained sand, showing moderately fining-upward sequence. Its color is gray to light-brownish gray. Many molluscan shell fragments and foraminiferal tests are included in this sand layer. Rip-up clasts, fragments of oyster shell and cobbles are included in the core A1. This sand layer erosionally covers underlying silt. Cracks are developed at the base of this sand layer except the core A1. The overlying sandy silt contains many plant fragments and large wood fragments. Especially in the core A4, plant fragments are laminated just above this sand layer.

OS-3: This sand layer is found in all cores. Its thicknesses are 1–6 cm and became thinner landward and the distal part of this layer has a patchy distribution. The thickness of the sand layer in each core is 4 cm (A0), 6 cm (A1), 4.5 cm (A2), 5 cm (A3), 1 cm (A4), the lens-shape of 2 cm or less (A5) and the lens-shape of 1 cm or less (A6). The sand layer in the core A6 consists of several sand lenses that distribute in the width of 5 cm. It is composed of fine to coarse grained sand, showing moderately fining-upward sequence. Its color is gray to light-brownish gray. In the seaward cores (A0, A1, A2), it is possible to divide the sand layer into two sections based on its internally stratification. The lower part is coarser than the upper one, and consists of poorly sorted coarse to medium-grained sand. The base of the lower part contains many gravels. The upper part mostly consists of medium grained sand. There are many gravels at the boundary between upper and lower part. Apart from these cores, this sand layer consists of poorly sorted coarse-grained sand and its basal part contains very coarse-grained sand. The sand layer erosionally covers underlying silt. The overlying silt contains plant fragments, but relatively few.

OS-4: This sand layer is found in all cores. Its thicknesses range from less than 5 mm to 6 cm and became thinner landward. The distal part of this layer has a patchy distribution. The thickness of the sand layer in each core is 2 cm (A0), 4 cm (A1), 6 cm (A2), 3 cm (A3), 1 cm (A4), less than 5 mm (A5) and the lens-shape of less than 5 mm (A6). This sand layer in the core A5 is missing in parts, and in the core A6 consists of several sand lenses that distribute in width of 1 cm. This sand layer is composed of fine to very coarse grained sand. It is dark gray to black. The sand layer in seaward cores (A0, A1, A2) has relatively coarser grain-size, shows moderately fining-upward sequence and includes rip-up clasts. Gravels are included in this sand layer of cores A0, A1, A2 and A3. In core A2, it has coarsest grain-size among all cores. The lower contact of this layer is not clear in many cases, and the underlying silt includes very fine to very coarse grained sand that is coarser in seaward cores than in landward cores. This sand layer has a gradational upper contact with the overlying silt. The overlying silt includes very coarse to coarse grained sand with plant fragments in cores A0, A1, A2 and A3, and very fine to fine-grained sand with plant fragments in other cores.

OS-5: This sand layer is found in all cores. Its thicknesses range from less than 1 cm to 18 cm. It becomes thinner landward and the distal part of this layer has a patchy distribution. The thickness of this sand layer in each core is 17 cm (A0), 18 cm (A1), 13 cm (A2), 7 cm (A3), 10 cm (A4), 4 cm (A5) and the lens-shape of less than 1 cm (A6). The sand layer in the core A6 consists of several sand lenses that distribute in width of 8 cm. The sand layer is composed of medium to very coarse grained sand with silt, including a few molluscan shells in the lower part. Its color is grayish black. This sand layer shows finer-grained landward sequence. Rip-up clasts and many pebbles are included in this sand layer of the core A0. The sand layer in the core A0 has three repetitive depositional phases that are combinations of very coarse grained sand and fine grained sand. Each phase seem to show a moderately fining-upward sequence. Additionally in the A2, A3 and A4 cores, this sand layer has two phases that are combinations of very coarse grained sand and fine grained sand. The sand layer in the A1 core shows coarsening-upward sequence and have many pebbles in the basal part. The lower contact of this layer is sharp in cores A1, A3, A4 and A6, and gradational in other cores. An erosion surface is present at the base of this sand layer in many cases and contacts the lower sand layer directly. The overlying silt includes very fine to very coarse grained

sand with plant fragments. In cores A2, A3 and A4, the sand layer has a gradational upper contact with the overlying silt.

OS-6: This sand layer is found in A0, A1, A2, A3 and A4 cores. Its thicknesses range from 5 cm to 22 cm and becomes thinner landward. The thickness of this sand layer in each core is 10 cm (A0), 18 cm (A1), 22 cm (A2), 15 cm (A3) and 5 cm (A4). It is composed of fine to very coarse grained sand, showing a general finer-grained landward sequence. It is light gray to grayish black. Two or three repetitive depositional phases, as the layer OS-5, are observed in all the cores. The molluscan shells and foraminiferal tests start to occur in the middle part of this sand layer, and their abundance increase downward. This sand layer erosionally covers underlying sandy silt including plant fragments. It has a sharp upper contact with the layer OS-5 in all cores except the core A3. There are many pebbles, which are derived from the layer OS-5, around the upper contact. Especially in the core A0, rip-up clasts are present. This sand layer in the core A3 has a gradational upper contact with the overlying silt. In the core A3, plant fragments are laminated just above this sand layer.

OS-8: This sand layer is found in all cores expect the core A6. In the core A6, there are several sand lenses that exist at the horizon which correspond to the layer OS-8 and which distribute in width of 3 cm. These sand lenses might therefore be the layer OS-8. Its thicknesses range from 2 cm to 17 cm. This sand layer becomes thinner landward. The thickness of this sand layer in each core is 17 cm (A0), 8 cm (A1; however, in this core it shows a patchy distribution upwards and gradually changes to the sandy silt, so it might be over 8 cm), 10 cm (A2), 17 cm (A3), 10 cm (A4) and 2 cm (A5). This sand layer is composed of very fine to medium grained sand, showing a fining-upward sequence. Its color is Light gray. Many molluscan shells and foraminiferal tests are included in this sand layer (thus, this sand layer is relatively whitish). The sand layer shows a finer-grained landward sequence. The sand layer displays internal stratification in the form of multiple silt-sand couplets. In the lowermost part, there is a relatively thick sand layer (around 4 cm). The upper part of this sand layer contains plant fragments. The sand layer erosionally covers underlying silt including plant fragments. There is colored mineral concentrated layer in the underlying silt.

OS-9: This sand layer is found in all cores. Its thickness ranges from 6 cm to 13 cm. The layer thickness in each core is 13 cm (A0), 9 cm (A1), 8 cm (A2), 9 cm (A3), 9 cm (A4), 10 cm (A5) and 6 cm (A6). The light gray colored sand layer is composed of fine to coarse grained sand, showing a moderately fining-upward sequence. Many molluscan shells and foraminiferal tests are included in this sand layer. It displays internal stratification in the form of multiple silt-sand couplets, as the layer OS-8. However, in core A2, uppermost sand layer of these couplets is coarsest and thickest. In core A6, the sand layer consists of a few lens-shaped sand layers in the upper part and a relatively thick sand layer (around 2 cm) in the lower part. Plant fragments are confirmed within interbedded silt of these couplets. This sand layer erosionally covers underlying silt. Cracks are developed at its base partly. This sand layer has a gradational upper contact with overlying silt.

OS-10: This sand layer is found in all cores. Its thicknesses range from 1 mm to 1.2 cm. The layer thickness in each core is 1.2 cm (A0), 1 cm (A1), two lens-shape layers of 3 mm (A2), 1 cm (A3), 1.2 cm (A4), 2 cm–1 mm (A5) and 5 mm (A6). The sand layer is composed of fine to medium grained sand and is dark gray. A few molluscan shells are included in this sand layer of cores A1 and A2. In cores A0, A1, A3 and A4, the sand layer consist of two sand layers (each 4 mm thick) and these sand layers intercalate silt. In other words, this sand layer consists of one and a half sand-silt couplets. In other cores, the sand layer consists of thin lenticular sand layers. The lower and upper contact is sharp. The overlying and underlying silt include a few plant fragments. In cores A0 and A1, the overlying silt includes very fine grained sand.

OS-11: This sand layer is found in cores A0, A1, A2, A3 and A4. Its thicknesses range from 1 mm to 5 mm. The layer thickness in each core is 1–5 mm (A0), 5 mm (A1), 5 mm (A2), 5–<1 mm (A3) and <5 mm (A4). The gray colored sand layer is composed of fine to medium grained sand. The lower and upper contact is sharp. The overlying and underlying silt includes plant fragments. Especially, the overlying silt layer includes many plant fragments. In core A0, it displays parallel alignment.

OS-12: This sand layer is found in cores A0, A1, A2 and A3. Its thicknesses range from 5 mm to 7 cm. The layer thickness in each core is 1.2 cm (A0), 8 cm–5 mm (A1; the distal part of this sand layer becomes thinner), 7 cm (A2) and 3 cm (A3). The dark gray colored sand layer is composed of fine to coarse grained sand. A few molluscan shells are included in the thick part of this sand layer in core A1. In cores A0, A2 and A3, the sand layer consists of two sand layers (around 2 mm–1 cm in thickness) showing a moderately fining-upward sequence, and these sand layers intercalate silt including plant fragments. In other words, this sand layer consists of one and a half sand-silt couplets. The lower and upper contacts are sharp. The overlying and underlying silt include plant fragments.

4.1.2. The middle part

This part is found in depths of 3.56–3.66 m in the core A5 and of 2.76–4.10 m in the core A6. It is composed of very fine to medium grained sand, including many marine molluscan shells and plant fragments. It is gray to light-grayish brown colored and there is an unconformable base at the bottom.

4.1.3. The lower part

This part is found only in the core A6 at depths of 4.10–5.70 m. Its thickness is about 1.6 m. This part corresponds to the Sakishima Formation. It is composed of poorly sorted, massive sand and sandy gravel, including pebbles (around 3 cm diameter). It is colored gray to bluish gray. The matrix shows a fining-upward sequence of medium to fine grained sand. Grain sizes of pebbles show fining-upward (3–0.5 cm diameter). This part is weathered overall.

4.2. Site B

Lithofacies of the obtained core in this area can be divided into two parts based on the sedimentary facies, i.e., the lower part (homogeneous marine clay) and the upper part (silt with organic fragments, intercalating around 10 sand or sandy gravel layers) (Fig. 3).

4.2.1. The upper part

This part constitutes the main part of cores, which is found at depths of 1.65–4.72 m. Its thickness is 3.07 m. It is composed of organic-rich silt and/or sandy silt, including plant fragments and is brownish black to dark brown. This part is overlain by an artificial bank used for cultivation.

Many sand layers are present in this part. These sand layers have a range in thickness from less than 1 cm to 13 cm. A colored mineral-bearing layer is present at depths of 300–302 cm. Based on lithofacies and stratigraphic position of the colored mineral concentrated layer, some of these sand layers are correlated with the OS series sand layers at site A. Detailed profiles of sand layers are described as follows (Fig. 3).

OS-1: This sand layer is found at depths of 231–244 cm. Its thickness is 13 cm. The sand layer is composed of poorly-sorted coarse-grained sand, showing a fining-upward sequence. Its color is black. Molluscan shell fragments, foraminiferal tests, gravels (2–3 cm in diameter) and rip-up clasts (2–3 cm in diameter) are included in this sand layer. This sand layer erosionally covers underlying silt. The overlying sandy silt includes many plant fragments, thin sand layers (2 mm–1 cm in thickness) and lens-shaped sand layers. The core B1 was excavated at almost the same site as the site of the core studied by Okahashi et al. (2001b). Furthermore its lithofacies are very similar to each other. Thus, this sand layer is correlated with the Layer B of Okahashi et al. (2001b) based on lithofacies and stratigraphic position.

OS-5: This sand layer is found at depths of 277–279 cm. Its thickness is only 2 cm. This thinness shows that this site is relatively far from the seashore. The gray colored sand layer is composed of fine to medium grained sand, showing a fining-upward sequence. This sand layer erosionally covers underlying silt. The overlying sandy silt includes many plant fragments. It is correlated with the Layer F of Okahashi et al. (2001b) based on lithofacies and stratigraphic position.

OS-8: This sand layer is found at depths of 289–290 cm and has a thickness of 1 cm. This sand layer is composed of fine to medium grained sand, including molluscan shell fragments and foraminiferal tests. Its color is light gray. Lower contact is sharp. Cracks are developed at the base of the sand layer. The overlying sandy silt includes lens-shaped sand layers (<1 cm in thickness). Plant fragments are concentrated just above the sand layer. There is a colored mineral concentrated layer in the underlying silt. This sand layer is correlated with the Layer H of Okahashi et al. (2001b) based on lithofacies and stratigraphic position.

335 cm depth: This sand layer is composed of a lens-shaped fine grained sand layer (1 cm in thickness).

394–396 cm depth: This sand layer is composed of four lens-shaped fine-medium grained sand layers including wood fragments (at 396 cm in depth; 3 cm in major axis).

399–400 cm depth: This sand layer is composed of a whitish gray colored fine-medium grained sand layer including lenses of sandy silt.

4.2.2. The lower part

This part was found in depths of 4.82–5.80 m. Its thickness is about 0.98 m. It is composed of homogeneous clay, including many molluscan shells, and is gray colored. The lens-shaped volcanic ash layer is found at the depth of 521–524 cm.

4.3. Site P

Stratigraphy of the obtained cores in this area consist of only one part (organic silt part). Cores P1 and P2 were excavated at the bottom of the pond. Distance between these sites is 3 m. Thus, the lithofacies of these cores are very similar to each other (Fig. 4).

4.3.1. Organic silt part

This part constitutes all parts of cores. It is composed

of organic silt and is colored dark brown to black. In the upper part, organic silt is sandy, poorly-sorted and sludged (0–90 cm.depth in P1; 0–80 cm depth in P2), and includes rubbles (around 5 cm in diameter; 31–47 cm.depth in P1; 35–47 cm depth in P2).

Many sand layers are present in the lower part of this part. These sand layers have a range in thickness from 1 to 16 cm. A colored mineral-concentrated layer is present at depths of 234–236 cm of the core P2. Based on lithofacies and stratigraphic position of the colored mineral concentrated layer, some of these sand layers are correlated with the OS series sand layers at site A, although several sand layers cannot be correlated with the OS series. Detailed profiles of sand layers are described as follows (Fig. 4).

OS-1: This sand layer is found at depths of 158–162 cm (P1) and 161–169 cm (P2). Its thicknesses are 4 cm (P1) and 8 cm (P2). The sand layer is composed of fine to coarse grained sand, including molluscan shell fragments and rip-up clasts. It is colored dark gray. The upper part of this sand layer shows a moderately fining-upward sequence. Grain size is relatively coarse at the bottom. This sand layer erosionally covers underlying silt. The overlying sandy silt includes many plant fragments.

OS-2: This sand layer is found at depths of 163–168 cm in the core P1. Its thickness is 5 cm. This sand layer is composed of fine to medium grained sand, including rip-up clasts and many molluscan shell fragments. It is colored grayish brown. This sand layer erosionally covers underlying silt. The overlying silt includes many plant fragments that are laminated. In the core P2, this sand layer is absent. This fact may suggest that this sand layer is eroded by the sand layer OS-1.

195–196 cm depth in the core P2: This sand layer is composed of gray colored medium grained sand including molluscan shell fragments and foraminiferal tests (1 cm in thickness) and intercalates with lens-shaped silt (2 mm in thickness).

OS-5: This sand layer is found at depths of 198–205 cm (P1) and 212–228 cm (P2). Its thicknesses are 7 cm (P1) and 16 cm (P2). The sand layer is composed of medium to very coarse grained sand with silt, including many gravels. It is colored grayish black. A few molluscan shell fragments are included in the lower part. This sand layer erosionally covers the lower sand layer (OS-8). The overlying silt includes plant fragments and very fine–very coarse grained sand. The upper contact of this sand layer is unclear in the core P1.

OS-8: This sand layer is found at depths of 205–208 cm (P1) and 228–230 cm (P2). Its thicknesses are 3 cm (P1) and 2 cm (P2). The sand layer is composed of medium sand, including molluscan shell fragments. It is colored dark gray. This sand layer erosionally covers underlying silt. Cracks are developed at the base of this sand layer. It has a sharp upper contact with the layer OS-5, showing erosion by the layer OS-5.

OS-9: This sand layer is found at depths of 217–223 cm (P1) and 260–265 cm (P2). Its thicknesses are 6 cm (P1) and 5 cm (P2). The sand layer is composed of fine to coarse grained sand, showing a moderately fining-upward sequence. It is colored gray. Many molluscan shell fragments are included. The middle part of this sand layer displays internal stratification in the form of multiple silt-sand couplets in the core P1. The middle part in the core P2 includes lens-shaped silt layers. This sand layer erosionally covers underlying silt. Cracks are developed at the base of this sand layer. The overlying silt includes plant fragments and very fine grained sand.

236–238 cm depth in the core P1: This sand layer is composed of dark-gray colored fine grained sand (2 cm in thickness). There is an erosional surface at the bottom. It has an unclear upper contact with the overlying silt including plant and biggish wood fragments.

245–255 cm depth in the core P1: This sand layer is composed of whitish gray colored fine–medium grained sand including molluscan shell fragments and silt. There is an erosional surface at the bottom. The sand layer consists of two sand layers intercalating very thin multiple sand-silt couplets. The overlying silt includes many plant fragments.

262–265 cm depth in the core P1: This sand layer is composed of dark gray colored very fine–fine grained sand, and consists of two thin sand layers (<1 cm in thickness), i.e., relatively coarse lower layer and finer upper layer, intercalating silt with plant fragments. There is a sharp bottom contact for each sand layer.

279–286 cm depth in the core P1: This sand layer is composed of dark brown colored fine grained sand, and consists of three thin sand layers (<1 cm in thickness) intercalating with silt with plant fragments. There is a sharp bottom contact for each sand layer.

284–296 cm depth in the core P2: This sand layer is composed of dark gray colored fine–medium grained sand including molluscan shell fragments and foraminiferal tests, and consists of unclear multiple sand–sandy silt couplets (sand-dominant in the lowermost 3 cm; silt-dominant in the upper part) including plant fragments in silt. Many plant fragments concentrate at the depth of 284 cm and wood fragments at the depth of 297 cm. This sand layer has an erosional surface at the bottom.

304–310 cm depth in the core P2: This sand layer is composed of dark gray colored medium–coarse grained sand (6 cm in thickness). There is lens-shaped silt at a

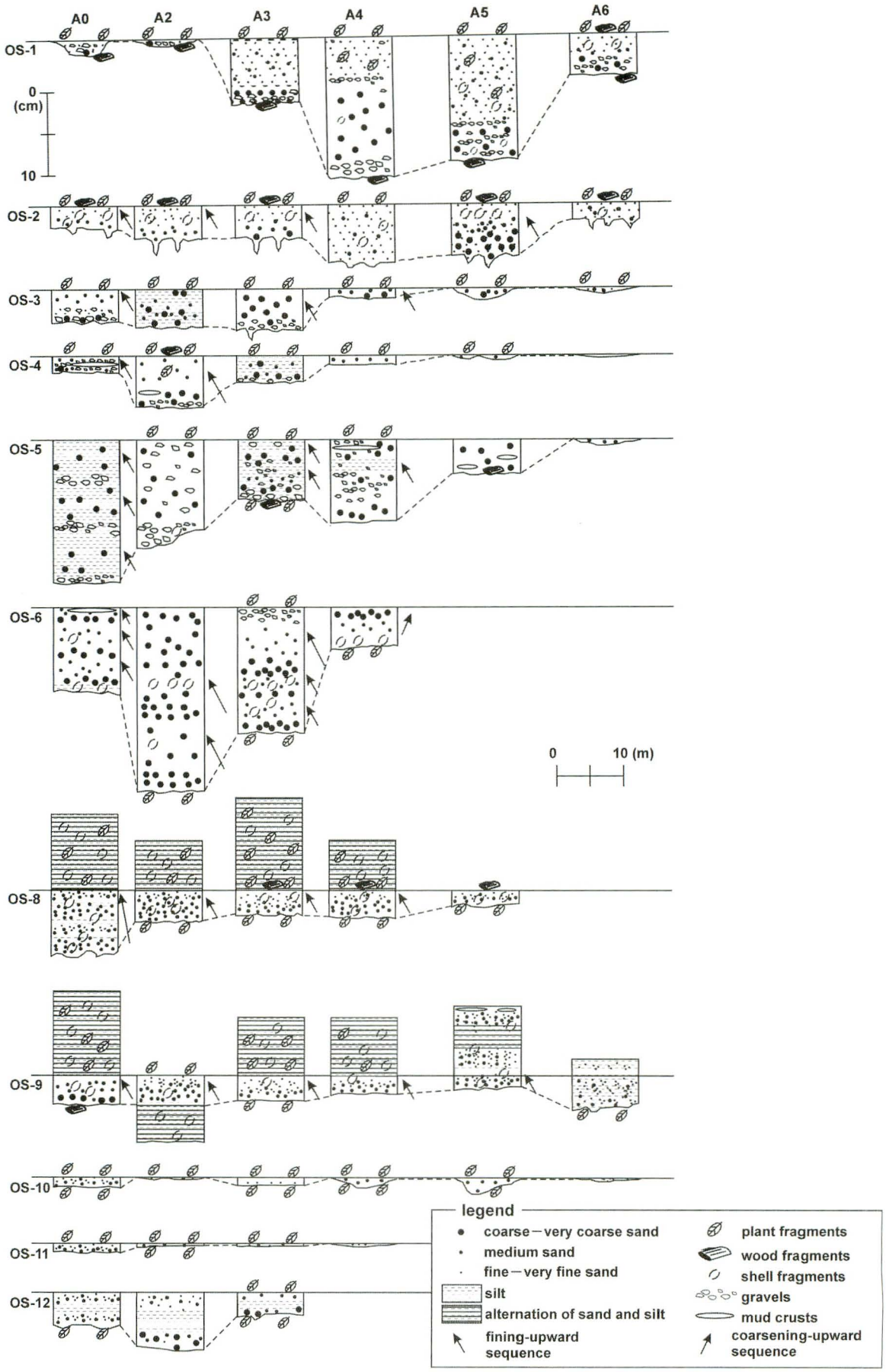

Fig. 5 Thickness, distribution and lithofacies of OS-series sand sheets in site A.

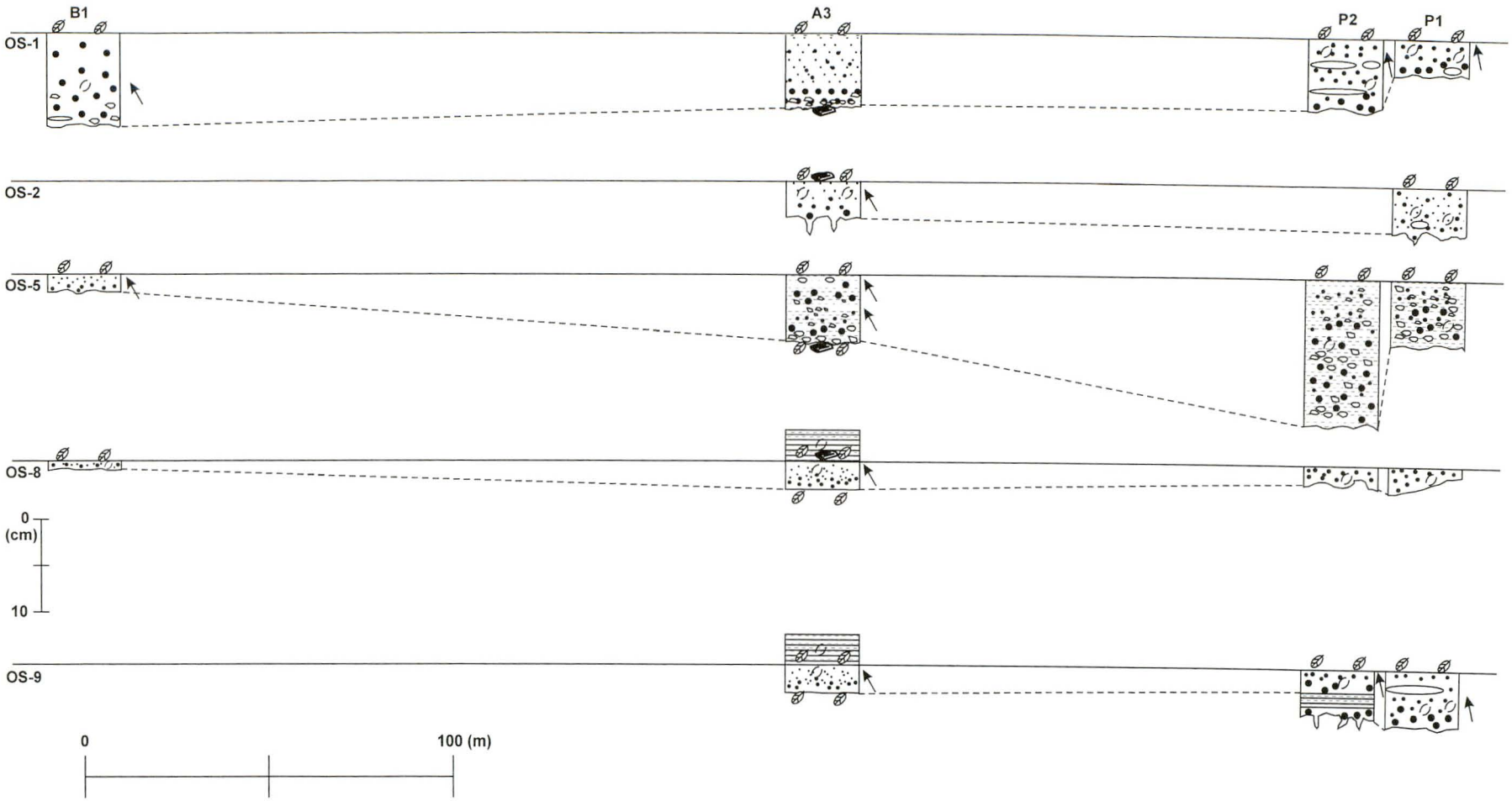

Fig. 6 Comparison of characters of OS-series sand sheets among sites.
Legend is shown in Fig. 5

depth of 308 cm. The upper part than lens-shaped silt shows a fining-upward sequence. This sand layer has an unclear upper contact with the overlying organic silt, and erosional surface and cracks at the bottom.

322–327 cm depth in the core P2: This sand layer is composed of gray colored medium–coarse grained sand (5 cm in thickness). There is lens-shaped silt at the depth of 324 cm and an erosional surface at the bottom.

Characters of sand layers at these three sites are summarized as follows. Each sand layer exists in organic silt and has an erosional surface at the bottom or sharp bottom contact. Plant fragments are concentrated just above each sand layer in most cases. Grain size of sand layers ranges from very fine sand to very coarse sand with gravel. Rip-up clasts, plant fragments, molluscan shell fragments and/or foraminiferal tests are included in many sand layers. Many sand layers in cores at site A have a wide-range and continuous distribution (Fig. 5). Furthermore, five sand layers (OS-1, 2, 5, 8 and 9) are correlated between more than two sites (Fig. 6). In site A, sand layers become thinner landward in many cases (OS-3, 4, 5, 6 and 8). Some sand layers (OS-1, 3, 5, 6, 8 and 9) consist of several sub-units showing a fining-upward sequence.

5. Radiocarbon dating

Sixteen radiocarbon ages of plants and woods were obtained by AMS method at Nagoya University Center for Chronological Research. Among them, six are from Mitamura et al (2001) and ten are new data. The radiocarbon ages were corrected for isotope fractionation with $\delta^{13}C$ value, and then were converted to calendar ages (cal yr BP) using the CALIB 4.3 (Stuiver et al., 1998). The results were shown in Table 1.

6. Discussions and conclusions

6.1. Temporal changes of depositional environments

Based on marine molluscan shells and lithofacies, the middle part of cores in site A and lower part of the core in site B are thought as the marine deposits (marine sand and marine clay respectively). Many marine and/or marine-brackish diatoms (e.g. *Tryblionella panduriformis, Cymatotheca weissflogii*) observed in core B1 (Hirose et al., 2002) also strongly suggests that this part consists of marine deposits. In the lower part of the core in site B, a volcanic ash layer exists. Mitamura et al. (2001) reported that this volcanic ash is correlated to the Kikai-Akahoya (K-Ah) Volcanic Ash, dated at ca. 7,300 cal yr BP (Fukusawa, 1995).

The organic silt (about 4–5 m thickness) constituting the main part of all cores had been deposited in all parts of the marsh. This part was divided into three zones at sites A and B (BI-III, AI-III) and five zones at site P (PI–PV) respectively on the basis of diatom analysis (see Fig. 7 and Hirose et al., 2002 for detail). Each diatom zone was characterized as follow (see Hirose et al., 2002 for detail): Zone I, the relatively abundant occurrence of fresh-water diatom (e.g., *Fragilaria exigua, Fragilaria densestriata*); Zone II, the dominance of marine-brackish diatom (e.g., *Fragilaria flavovirens, Fragilaria brevistriata*) and few occurrence or absence of fresh-water diatom; Zone III, the dominance of marine-brackish diatom (e.g., *Fragilaria flavovirens, Fragilaria brevistriata*) and the occurrence of *Fragilaria pinnata* var. *pinnata* (fresh-water diatom); Zone IV, the dominance of unique fresh-water species (i.e., *Nitzschia frustulum, Navicula accomoda*) and very few occurrence of marine- brackish diatom; Zone V, diverse fresh-water species (e.g., *Fragilaria exigua, Fragilaria pinnata* var. pinnata, *Fragilaria densestriata*).

Table 1 List of radiocarbon ages.

Core	Depth(cm)	Sample	^{14}C age(^{14}C yr BP)	Error (1sigma)	Calibrated age (cal yr BP)	Lab. Code	Reference
A5	243	wood	3005	±30	3230	NUTA-2077	Mitamura et al. (2001)
A5	337	wood	5435	±40	6220	NUTA-2078	Mitamura et al. (2001)
B1	197	wood	800	±30	7075	NUTA-2085	Mitamura et al. (2001)
B1	308	cone	3325	±30	3500	NUTA-2083	Mitamura et al. (2001)
B1	396	wood	5795	±35	6595	NUTA-2086	Mitamura et al. (2001)
B1	496	wood	5950	±35	6780	NUTA-2084	Mitamura et al. (2001)
A6	105	wood	1085	±25	970	NUTA2-5314	this study
A6	128	wood	1705	±25	1590	NUTA2-5315	this study
A6	130	wood	1520	±25	1410	NUTA2-5316	this study
A6	136	wood	1685	±25	1565	NUTA2-5317	this study
A6	140	wood	1630	±25	1530	NUTA2-5318	this study
A6	193	wood	3655	±30	3975	NUTA2-5319	this study
A6	276	wood	5785	±30	6625	NUTA2-5323	this study
A6	351	wood	6040	±30	6685	NUTA2-5324	this study
A6	366	wood	6300	±30	7250	NUTA2-5325	this study
A6	370	wood	6400	±30	7315	NUTA2-5326	this study

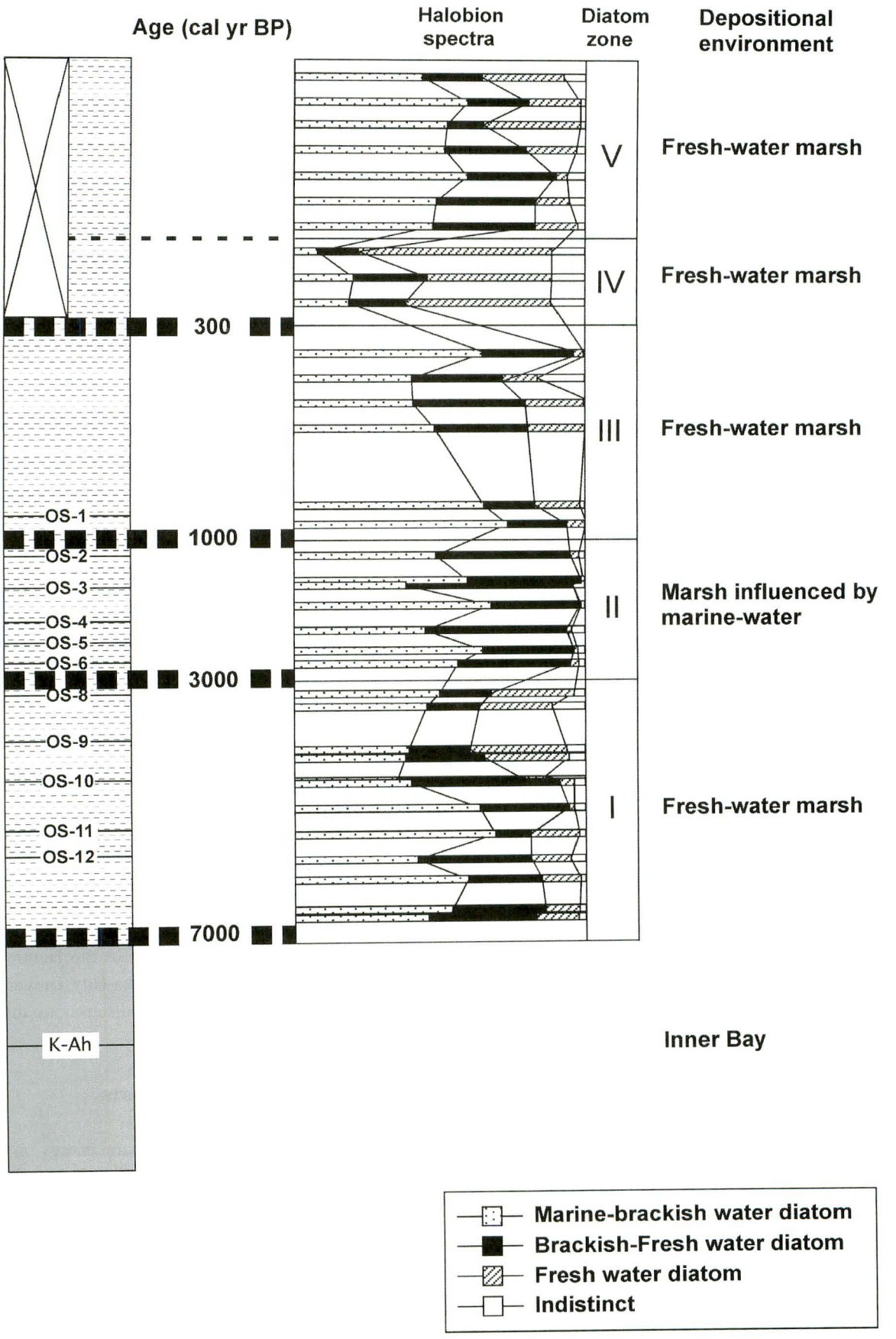

Fig. 7 Temporal changes of depositional environment and summary of the stratigraphy and diatom analysis of the studied area. Diatom data from Hirose et al. (2002).

Based on the above-mentioned evidences and radiocarbon ages, temporal changes in depositional environments of the studied area are summarized as follows: Around 7,000 cal yr BP, the studied area had been under marine (inner bay) environment. After that, the influence of fresh water had increased, and then the studied area had been a fresh-water marsh during ca. 6,500–3,000 cal yr BP. During ca. 3,000–1,000 cal yr BP, influence of marine water had increased. Because this period corresponds to the middle part of the organic silt layer that contains many and thick sand layers (see Figs. 2–4 and 7), this increase of marine-water influence may be due to tsunami (see below for detailed discussion that sand layers is tsunami deposits), i.e., marine water may be provided to the marsh by tsunami and persistent for a relatively long time. After ca. 1,000 cal yr BP, the studied area had been under a fresh-water environment again. Because this period corresponds to the upper part of the organic silt layer that contain relatively few sand layers (see Figs. 2–4 and 7), this decrease of marine-water influence may be due to the decrease of tsunami inundations or magnitude. Unique fresh-water species in Zone IV suggests the paddy cultivation during the Edo Period – the beginning of the Showa Period. After that, the studied area became a fresh-water marsh again, because of the cessation of the paddy cultivation.

Artificial fill (about 1 m thickness) is distributed on the surface of the marsh except site P.

6.2. Origin of sand layers

Over ten sand layers are intercalated in the organic silt. Contacts between these sand layers and lower beds are sharp and commonly erosional. Some of the thick sand layers display multiple fining-upward sequences or sand-silt combinations. Many sand layers became thinner and fine-grained landward (see Fig. 5), and contain foraminiferal tests. Molluscan shell fragments are common. Plant fragments are abundant in the silt immediately overlying the sand layers in most cases. As mentioned above, these sand layers, that are intercalated in fine coastal marsh deposits (i.e., organic silt), show sudden lithofacies changes. Furthermore, there is no large river around the studied area, i.e., coarse sediments are not deposited in the studied marsh under normal conditions. These results and evidences strongly suggest that sands were transported to the studied marsh (i.e., sand layers were formed) by some kind of events.

One of these events, that can cause the above-mentioned sand deposition, is tsunami. Tsunami deposits commonly consist of sandy sediments or sandy gravel, display fining-upward sequences, become thinner and finer-grained landward and are widespread (Atwater et al., 1995). Microfossils of marine-origin are common in tsunami deposits (Benson, et al., 1997). Outside of these, the following characters have been recognized: erosional surface at the bottom; plant fragments (e.g., woods and leaves) in the upper part and in the fine deposit immediately overlying tsunami deposit (Clague and Bobrowsky, 1994; Benson et al., 1997). Event deposits (i.e., sand layers) in this study display similar characters to tsunami deposit as mentioned above. Furthermore, Okahashi et al. (2002) reported foraminiferal assemblages in the sand layers of core A1. Among them, some species live in the area that has a great water-depth (50–100 m water depth and/or 100–150 m water depth). This result strongly suggests that these event deposit were formed by tsunamis, because transportation of foraminiferal tests from such deep area to studied marsh by the normal wave is probably impossible.

Acknowledgements

We are grateful to Dr. Tsuyoshi Haraguchi (Osaka City University), and staffs of Fukken Co. Ltd. for sampling by "Geo-slicer", Dr. Toshio Nakamura (Nagoya University) for radiocarbon dating, and Dr. Wataru Maejima (Osaka City University) for sedimentological advice. We appreciate assistance of sampling by Dr. Masayuki Hyodo (Kobe University), Dr. Takashi Uchiyama (Yamanashi Institute of Environmental Sciences), Dr. Mieko Uchiyama (National Institute of Advanced Industrial Science and Technology) and Ms. Akiko Murakami (Osaka City University). Reviews by Dr. Hisao Kumai (Osaka City University) and Dr. Keiji Takemura (Kyoto University) helped us to improve the manuscript. Graduate students of the Natural History of Anthropogene Laboratory, Osaka City University, provide us various advices and useful discussions throughout the course of the present study.

References

Aida, I. (1988) Cumulative tsunami energy on the Japanese coast as a measure of long-term tsunami hazard. *Journal of the Seismological Society of Japan, 2nd series (Zisin 2-syu)*, **41**, 573–581. (in Japanese with English abstract)

Atwater, B. F. (1987) Evidence for great Holocene earthquakes along the outer coast of Washington State. *Science*, **236**, 942–944.

Atwater, B. F., Nelson, A. R., Clague, J. J., Carver, G. A., Yamaguchi, D. K., Bobrowsky, P. T., Bourgeios, J.,

Darienzo, M. E., Grant, W. C., Hemphill-Haley, E., Kelsey, H. M., Jacoby, G. C., Nishenko, S. P., Palmer, S. P., Peterson, C. D. and Reinhart, M. A. (1995) Coastal geologic evidence for past great earthquakes at the Cascadia Subduction Zone. *Earthquake Spectra*, **11**, 1–18.

Benson, B. E., Grimm, K. A. and Clague, J. J. (1997) Tsunami deposits beneath tidal marshes on northwestern Vancouver Island, British Columbia. *Quaternary Research*, **48**, 192–204.

Compilation room of "History of Toba City" (1991) *History of Toba City*, Toba City Office, 1347 pp. (in Japanese)

Clague, J. J. and Bobrowsky, P. T. (1994) Evidence for a large earthquake and tsunami 100–400 years ago on western Vancouver Island, British Columbia. *Quaternary Research*, **41**, 176–184.

Dawson, A. G., Hindson, R., Andrade, C., Freitas, C., Parish, R. and Bateman, M. (1995) Tsunami sedimentation associated with the Lisbon earthquake of 1 November AD 1755: Boca do Rio, Algarve, Portugal. *The Holocene*, **5**, 209–215.

Fujiwara, O., Masuda, F., Sakai, T., Fuse, K. and Saito, A. (1997) Tsunami deposits in Holocene bay-floor mud and the uplift history of the Boso and Miura Peninsulas. *The Quaternary Research (Daiyonki-kenkyu)*, **36**, 73–86. (in Japanese with English abstract)

Fujiwara, O., Masuda, F., Sakai, T., Irizuki, T. and Fuse, K. (1999) Holocene tsunami deposits detected by drilling in drowned valleys of the Boso and Miura Peninsulas. *The Quaternary Research (Daiyonki-kenkyu)*, **38**, 41–58. (in Japanese with English abstract)

Fujiwara, O., Masuda, F., Sakai, T., Irizuki, T. and Fuse, K. (2000) Tsunami deposits in Holocene bay mud in southern Kanto region, Pacific coast of central Japan. *Sedimentary Geology*, **135**, 219–230.

Fukusawa, H. (1995) Non-glacial varved lake sediment as a natural timekeeper and detector on environmental changes. *The Quaternary Research (Daiyonki-kenkyu)*, **34**, 135–149. (in Japanese with English abstract)

Hirose, K., Gotoh, T., Mitamura, M., Okahashi, H. and Yoshikawa, S. (2002) Event deposits and paleoenvironmental changes in the marsh deposit at Osatsu, Toba City, Central Japan. *Chikyu Monthly*, **24**, 692–697. (in Japanese)

Minoura, K., Nakaya, S. and Sato, H. (1987) Traces of tsunami recorded in lake deposits: Examples from Jusan, Shiura-nada, Aomori. *Journal of the Seismological Society of Japan, 2nd series (Zisin 2-syu)*, **40**, 183–196. (in Japanese with English abstract)

Mitamura, M., Okahashi, H., Hirose, K., Yoshikawa, S., Uchiyama, M., Nakamura, T. and Haraguchi, T. (2001) Event deposit and ^{14}C age preserved in coastal marsh in Osatsu, Toba, central Japan. *Proceedings of the 11th Symposium on Geo-Environments and Geo-Technics*, 321–326. (in Japanese with English abstract)

Nanayama, F., Satake, K., Furukawa, R., Shimokawa, K., Atwater, B.F., Shigeno, K. and Yamaki S. (2003) Unusually large earthquakes inferred from tsunami deposits along the Kuril trench. *Nature*, **424**, 660–663.

Nakata, T. and Shimazaki, K. (1997) Geo-slicer, a newly invented soil sampler, for high-resolution active fault studies. *Journal of Geography*, **106**, 59–69. (in Japanese with English abstract)

Okahashi, H., Akimoto, K., Mitamura, M., Hirose, K., Yoshikawa, S., Uchiyama, M. and Haraguchi, T. (2001a) Event deposits preserved in coastal marsh at Osatsu, Toba, central Japan (2). *Programme and Abstracts of the Annual Meeting of Japan Association for Quaternary Research*, 31, 46–47. (in Japanese)

Okahashi, H., Yoshikawa, S., Mitamura, M., Hyodo, M., Uchiyama, T., Uchiyama, M. and Haraguchi, T. (2001b) Tsunami deposits of Tokai earthquakes preserved in a coastal marsh sequence at Osatsu, Toba, central Japan, and their magnetochronological dates. *The Quaternary Research (Daiyonki-kenkyu)*, **40**, 193–202. (in Japanese with English abstract)

Okahashi, H., Akimoto, K., Mitamura, M., Hirose, K., Yasuhara, M. and Yoshikawa, S. (2002) Event deposits preserved in coastal marsh at Osatsu, Toba, central Japan: recognition of tsunami deposit on the basis of foraminifera analysis. *Chikyu Monthly*, **24**, 698–703. (in Japanese)

Otsuka, Y. (1928a) Isobe-mura fukin no sizen-chirigakuteki-chisi no ichibu no kenkyu (jyo) (Physical geographic geohistory around Isobe Village, part 1). *Geographical Review of Japan (Chirigaku-hyoron)*, **4**, 175–189. (in japanese)

Otsuka, Y. (1928b) Isobe-mura fukin no sizen-chirigakuteki-chisi no ichibu no kenkyu (ge) (Physical geographic geohistory around Isobe Village, part 2). *Geographical Review of Japan (Chirigaku-hyoron)*, **4**, 284–297. (in japanese)

Stuiver, M., Reimer, P., Bard, E., Beck, J. W., Burr, G. S., Hughen, K. A., Kromer, B., McCormac, G., van der Plincht, J. and Spurk, M. (1998) INTERCAL98 radiocarbon age calibration, 24,000–0 cal BP. *Radiocarbon*, **40**, 1041–1083.

Tsuji, Y. (1999) History of tsunami damage at Kuzaki

Village, Toba City, Mie Prefecture. *Historical Earthquake (Rekishi-zisin)*, **15**, 65–71. (in japanese)

Tsuji, Y., Okamura, M., Matsuoka, H. and Murakami, Y. (1998) Tsunami trace survey in the deposits of Lake Hamana. *Historical Earthquake (Rekishi-zisin)*, **14**, 101–113. (in japanese)

Tsuji, Y., Goto, T., Okamura, M., Matsuoka, H. and Han, S.S. (2001) Historical and pre-historical tsunami traces in the sediments of Lake Ooike, Sukari-Ura, Owase City, Mie Prefecture. *DCRC Tsunami Engineering Technical Report*, **18**, 11–14. (in japanese)

Tsuji, Y., Okamura, M., Matsuoka, H., Goto, T. and Han, S.S. (2002) Historical and pre-historical tsunami traces in the sediments of Lake Ooike (Sukari-Ura, Owase City, Mie Prefecture) and Lake Suwaike (Kii-Nagashima City). *Chikyu Monthly*, **24**, 743–747. (in japanese)

Watanabe, H. (1998) *Comprehensive List of Tsunamis to Hit the Japanese Islands*. Tokyo University Press, 238 pp. (in Japanese)

Yamagiwa, N and Saka, Y. (1967) Mesozoic and Paleozoic in eastern part of Shima Peninsula. *The 74th Annual Meeting of the Geological Society of Japan Excursion Guidebook*, **5**, 24pp. (in Japanese)

Yoshikawa, S., Okahashi, H., Mitamura, M., Hirose, K. and Uchiyama, M. (2003) Event stratigraphy of Holocene sediments in Osatsu, Toba, central Japan. *Proceedings of the 13th Symposium on Geo-Environments and Geo-Technics*, 377–382. (in Japanese with English abstract)

Manuscript received August 31, 2004.
Revised manuscript accepted November 15, 2004.